Response to reviewer #1:

Dear reviewer,

Thank you very much for a constructive and insightful review. We have addressed all your comments and we believe this has improved the paper significantly. We hope that you agree and that our modifications are to your satisfaction.

Below we have copied out your comments in black and inserted our response in blue type.

Regards,

Einar (on behalf of the authors)

The manuscript would benefit from some further discussion for the general reader that better situates the findings in the context of the published literature and suggests implications for the broader scientific community, rather than simply for the development of neXtSIM. For example, why is it the mono/multifractal scaling interesting? Does the work suggest parametrizations that could be used in traditional climate/sea ice models? This comment is merely a suggestion and the authors are not required to address it.

This is a very insightful comment as it goes to the heart of the motivation of the paper. Both this comment and comments by the other reviewer show that the paper's motivation needs to be stated more clearly - something we have tried to do in the modified manuscript.

Major comments
I find the exclusion of the Beaufort Sea from the model-observation comparison to be poorly motivated. The model-observation comparison does not seem fair if the authors exclude regions where the comparison is poor. The authors need to motivate the exclusion of this region better and quantify to what extent the exclusion of the region affects their conclusions, or refrain from excluding it in their analysis.

Indeed, the motivation for excluding the Beaufort Sea was not clear in the original submission. Our main reason for doing so was an apparent inconsistency in the observations between the Beaufort Sea and the rest of the Central Arctic. Further work on this issue - following this review - has, however, made it clear to us that excluding the Beaufort Sea is not well justified. In the revised text all analysis and comparisons are made on the "Arctic" and "Central Arctic" regions only.

Data availability – According to The Cryosphere data policy, 'Authors are required to provide a statement on how their underlying research data can be accessed.' This is missing from the manuscript.

We've added this to the revised manuscript.

Line-by-line comments

L7 Wasn't the Central Arctic region chosen to avoid the presence of polynyas?

It should have said wider Arctic - this has been corrected in the revised text

L18 'In particular . . .' – add citation(s)

Done

L19 'Leads . . . are a much more temporally and spatially clustered gateways' – this is unclear, please revise

We've rewritten the sentence as "Leads in the centre of the Arctic Basin, on the other hand, are much more difficult to study because they are much narrower and shorter-lived than polynyas, and at the same time can form anywhere in the Arctic Basin."

L25 'causes' .. 'causing' – repetitive, rephrase

Changed 'causes' to 'drives'

L32 Missing parentheses

Fixed

L33 What area did the satellite image cover?

It was a 60x66 km2 image, we've added this to the text.

L36 'accurately reproduce the properties of lead fraction statistics' - add citation(s)

We've rewritten this statement to be more accurate and added references

L43 In what situations does the mixed layer deepen in response to brine rejection? My understanding is that this is what occurs in low resolution models. Barthélemy et al. (2015) (https://doi.org/10.1016/j.ocemod.2014.12.009) could be cited here.

The mixed layer shoals when (relative) ice velocity is low and the brine forms a plume that sinks to the bottom of the mixed layer. When the ice velocity is high the shear induces mixing of the brine which in turns causes a deepening of the mixed layer. In (most) low-resolution ocean models the brine is released uniformly into the first ocean layer causing mixing and deepening of the mixed layer - similar to the high-ice-velocity regime. Nguyen et al showed that releasing the brine at the bottom of the mixed layer improves the simulation. This is described in the text, although we have modified it slightly to make it clearer.

We were not aware of the Barthélemy paper, but it was very interesting to see the importance of including both the low- and high-velocity regimes. So we've added a reference to that as well. Thank you for pointing it out.

L48 'is actively being researched' – add citation(s)

Done

L49 'Lead formation is closely linked . . .' – add citation(s)

This sentence was poorly formulated. We've reformulated it to read "When sea ice deforms ridges and leads are formed." - which doesn't require a citation.

L54 Suggest defining multifractality here.

We have added a discussion of the relevance of (multi)fractality here.

L55 'This fundamental property . . .' This sentence needs more explanation for the general reader.

We've removed this sentence in favour of the more detailed discussion added.

L74 Please provide more details on the slab ocean. Does it include any representation of ocean currents? How might the simplicity of the modelling configuration affect results?

We intentionally didn't go into much detail about the model - including the slab ocean - since this is presented in more detail in Rampal et al (2019) and Rampal et al (2016). We did still add the sentence "Oceanic heat loss results in lowering of the slab ocean temperature, which may be compensated for by new-ice formation and

nudging of the slab ocean layer temperature to reanalysis results." to the text and hope you find it sufficient to address your comment.
As for how using a slab ocean affects the results then we expect this to be minor. We expect a larger contribution from the atmosphere in this respect, and that is mentioned in the discussion. To address your comment we've added a few sentences to this effect in the discussion section.

L95 Define 'node' and 'cohesion'

'Nodal spacing' was left over from a previous version of the manuscript. The correct phrasing is simply '12.5 and 25 km resolution', and we have changed this in the revised manuscript. Mentioning the cohesion at this point borders on being too precise, in our opinion and we prefer to refer to the discussion in Bouillon and Rampal w.r.t. scaling of cohesion. We have slightly reformulated and rephrased to make this clearer.

L99 'The deficiencies of the linear viscous model are well known' – add citation(s)

Done

L109 How is it an improvement?

The new product fixes an overestimation of the lead fraction present in the original. We've added a sentence to that effect in the text.

L126 Why are the heat flux magnitudes provided as snapshots rather than daily means?

They are not - this was left over from an earlier version of the paper. The heat fluxes and lead fractions are both daily means.

L154 Reword 'for future works' to 'in future work'

Done

L167 'that gives good statistics.' What does this mean?

It just means that it gives the same slope of the PDF, as per the latter part of the sentence. It now reads "We, therefore, choose a threshold thickness for the model that has the same slope of the PDF as the observed one, as shown below."

L168 Why not simply use a threshold of 10 cm? How much does the choice of threshold affect the results?

We wanted to see if we could deduce the appropriate threshold from the model statistics. The fact that the two are very close shows that the processes in the model are a reasonable reproduction of those in reality. Having done this it doesn't matter much which value we use for the comparison, the results are essentially the same. The paper also says that variations of the threshold of about 1 cm give the same results.
Note, however, that the 10 cm threshold is more of an educated guess and probably not a fixed threshold anyway - there is also a dependence on emissivity, frost flowers, and probably other factors as well. Since the 10 cm threshold is a very rough estimate we see no reason to prefer that over the model deduced threshold of 9.1 cm.

L182 Why do you think the model does not capture this?

We don't exclude the Beaufort Sea anymore, so this comment is not relevant.

Fig. 1 caption – define the red dashed lines. 'read' -> 'red'

The dashed line was what we exclude as the Beaufort Sea, but this is not relevant anymore.

L191 'excellent agreement' The figure is in log space, so some of the model- observation differences seem not insubstantial.

Indeed this was maybe overly enthusiastic wording. We go into more detail below about the model-observation differences to show that the observation shortcomings are such that it's hard to say to what extent the differences are indeed substantial. We, therefore, replaced 'excellent' with 'good' and added a sentence highlighting that the agreement between model and reality is probably much better than the comparison in the figure seems to indicate at a first glance.

Fig. 2 caption – are these lines excluding the Beaufort Sea? Typo in 'Arctic'

Yes, but as we don't exclude the Beaufort Sea anymore, so this comment is not relevant.

L210 What is 'proper' spatial scaling?

We've removed the word 'proper' - it should not have been there.

L275 'after some algebra' – this wording is too casual for a journal article

We've removed the phrase 'after some algebra'

L315 Reword 'this model shortcomings' to 'these model shortcomings'

Done

Response to reviewer #2 (Nils Hutter):

Dear Nils,

Thank you very much for a constructive and insightful review. We have addressed all your comments and we believe this has improved the paper significantly. We hope that you agree and that our modifications are to your satisfaction.

Below we have copied out your comments in black and inserted our response in blue type.

Regards,

Einar (on behalf of the authors)

General comment:
The authors choose rather complex statistical tools by analysing the heavy-tails of PDFs and the spatial scaling. These methods are appropriate to study the localisation of lead density and simulated heat flux, which is the main topic of the manuscript. However, a comparison of the spatial distribution of lead density as done in Wang et al. (2016) and Hutter & Losch (2020) is missing, although all data would be available for that. In Fig. 1 such a comparison is made for a snapshot of a single day. I recommend to add a comparison of spatial distribution of lead-density for the entire winter analysed in this paper (maybe replacing Fig. 1). In doing so, the model evaluation of this manuscript would be more comprehensive by showing that the model (might be)/is able to reproduce the large-scale spatial distribution and the strong localisation of lead-density.

Indeed, we have not made the kind of spatial distribution analysis that Wang et al and Hutter and Losch did. This would indeed be an interesting additional metric for a model-observations comparison, but we feel that adding it to the present paper would not be appropriate. The reason being that in this paper we are introducing the notion of using spatial scaling analysis to investigate lead fraction patterns. This is motivated by the spatial scaling we see in deformation rates, as we know that lead formation is closely linked to deformation.

In this paper, we show that both observed and modelled lead fraction patterns demonstrate spatial scaling and we then use the model to show that the (modelled but unobserved) heat-flux patterns also demonstrate spatial scaling. The model-observations comparison is therefore only there so that we can with some confidence say that there is likely also a spatial scaling of the heat fluxes in reality.

Adding the spatial distribution analysis, as suggested, would therefore not add to the central theme of the paper - which should be the spatial scaling of lead fraction and heat fluxes. We feel that adding an arguably parallel discussion to the paper in this manner would not be beneficial for the paper, but make it less focused and more difficult to follow. We therefore respectfully decline to follow the reviewer's recommendation on this point. We do, however, feel that this comment, together with one of the other reviewer's, makes it clear that the

introduction and motivation of the paper needs to be improved - something that we have attempted to do in the revised manuscript.

Specific comments:

P2, line 32: “Andreas and Cash (1999); Esau (2007)” - wrong citation style

Fixed

P2, line 35: “including smaller leads increased by 55% the total estimated heat flux” - including smaller leads increased the total estimated heat flux by 55%.

Fixed

P2, line 35-37: I assume that the magnitude of the overall heat flux is adjusted by the tuning of thermodynamic parameters in coarse resolution climate models. However the spatial distribution and local magnitude might be off, if leads are not resolved in these models. Please clarify.

You are right. We have changed under-represented to misrepresented, which is more appropriate.

P2, line 48-49: “the statistical properties of leads in large-scale sea-ice models have not yet been shown to be robustly reproduced” - How about Wang et al. (2016) and Hutter & Losch (2020). Wang et al. (2016) shows agreement in the lead density in the Arctic between a model simulations and satellite observations. Hutter & Losch (2020) show that multiple spatial and temporal properties of LKFs, which are leads and pressure ridges, observed from satellite are matched by large-scale sea-ice simulations.

We have now included those references in the text. The point we wanted to make was that models that are normally used to study the Arctic have neither the resolution nor the numerics necessary to resolve these features. This is made clearer in the revised manuscript.

P2, line 61: “Section 2.1” - Section 2.1 presents only the model set-up. Please refer to Section 2.

Fixed

P3, line 61-70: This paragraph reads a bit wordy. Maybe consider to rephrase it.

We have rewritten parts of this and hope that it reads better now.

P3, line 83: “model mesh” - Model mesh or the mesh to which the model output is interpolated?

The model mesh. We have rewritten this sentence slightly to make this clearer.

P4, line 1-2: Not clear, from which data product concentration and from which product thickness is taken. Please clarify.

This is clarified in the revised text

P5, l 125 “order” - order -> orders

Fixed

P5, l 136: “2011” - 2011 vs model year 2007? In the model description it is written that the model is ran for winter 2007, later on in the paper you evaluate only the year 2011. Please clarify. Does this sentence anyways not rather belong to the results section?

It was supposed to say 2007 and we’ve fixed that (here and in several other places). We used 2011 in a previous version of the paper. We think that the sentence belongs here because it illustrates the method of using averages of JFM and does not address the results. The reference to figures 2 and 4 is for illustrative purposes and the figures are only discussed in the results section.

P5, l150: “PÌD âLij L−β(0)” - Supposing x_bar should represent the mean, it should be

beta(q=1). For q=0 no scaling should be observable, if equation (2) is used (xˆ0=1 for all samples).

Yes, \bar{x} is the mean and it should be \beta(1), not \beta(0). We've fixed this.

P6, l152: "Stern et al. (2018) argue that this method provides a reasonably accurate estimate of the power-law fit." - In addition, Stern et al. (2018) argue that no matter what method is used for estimate of the power-law exponents a goodness-of-the-fit test like in Clauset et al. (2009) should be performed. Please clarify, if you do such a test, or why it is not necessary in this case.

P6, l153: "might provide" - Replace by "provides". Both Stern et al. (2018) and Clauset et al. (2009) say it provides better estimates. Given that the method is computationally not much more expensive, it is unclear to me, why you choose to use a more inaccurate method.

For the two points above: The second half of this paragraph was wrong. The MLE method of Clauset et al is to estimate if the PDF follows a power law, but this is not our concern here. We know that the PDF has a "fat" tail (doesn't need to be a power-law) and then we can reasonably expect there to be a scaling relationship - which we do find. We've removed the erroneous portion of the paragraph and slightly rewritten the surrounding text without changing its contents or meaning.

P6, l171-172: "It is important to note that the simulated lead fraction is not strictly a lead fraction as it includes all open water areas, including polynyas (cf figure 1)." - How about using a smoothened concentration field to mask large open-water areas as around Svalbard?

If we're doing that we would essentially be fabricating data since the smoothed field would have very different characteristics from the rest of the field.

P6, L 177: "showing a deviation from linearity at around 70%" - I can not see a clear deviation. Is it due to the dashed line style. An annotation to the plot could help to point the reader to what you mean.

This was not very clear in the original submission. But as we don't exclude the Beaufort Sea anymore, so this comment is no longer relevant.

P6, l178: "When excluding this region, the observations also show a linear decrease (Fig. 2, solid blue line)." - This does not fit to the caption of the Figure2 (dashed for "Arctic" and solid for "Central Arctic").

We've fixed the caption, which was wrong.

P6, l 182: "However, we suspect that the large number of small leads forming there may result in increased noise in the lead fraction product (see Fig.1) and an overestimation of the large lead fractions." - Not clear to me. Please be more specific why more small leads lead to an overestimation of the lead fraction product. Or do you mean that by having many small leads the lead fraction increases, but the model does not resolve these small leads and therefore shows lower lead fractions?

Indeed, the motivation for excluding the Beaufort Sea was not clear in the original submission. Our main reason for doing so was an apparent inconsistency in the observations between the Beaufort Sea and the rest of the Central Arctic. Further work on this issue, following this review, has, however, made it clear to us that excluding the Beaufort Sea is not well justified. In the revised text all analysis and comparisons are made on the "Arctic" and "Central Arctic" regions only.

P8, l197: "than 20%" - Add (note shown) or reference to figure.

This refers to the discussion in the paragraph above, so we've added "(see above)" to the text.

P8, l 203: "strong indicator" - Be cautious, even if the scaling is right, the regional distributions could be off, i.e. high lead fractions found close to the coast or in Beaufort sea in observations could be reproduced by the model in different regions. To clarify this, please be more specific what you mean with lead-fraction patterns in the text.

It is right that our use of the words “lead-fraction patterns” is too broad and not supported by our results. We have therefore rephrased the sentence to read “... strong indicator that the model is simulating lead formation in a physical and realistic manner …”

P11, l 243: “In addition to these differences in the scaling, there also seems to be a difference in the nature of the structure function, depending on the model resolution” - Please also discuss the change in structure function for the lead fraction. It appears that the linear fit is not appropriate to fit the structure function of the coarse resolution models (The fit does not pass the uncertainty interval for q=1).

This is true and we have noted it now.

P13, l267-269: “We also assume that the closing is directly proportional to the area of the polynya since most of the heat loss and ice formation happens over open water.” - This assumption is not clear: I agree that ice formation is larger over open water, but if a polynya is formed instantaneously the entire area of the polynya starts to freeze at the same time. Please clarify.

This was indeed not clear enough in the initial submission. The point is that we can assume that the closing rate is directly proportional to the area of the polynya since the total heat loss and total ice formation can be assumed to be proportional to the area of open water. This leads to the differential equation and the rest of this simplistic model. We’ve modified the text to be more precise.

P14, l 219: “figure 4” - Please reference the subfigure for clarity.

Done

P15, l300-308: “This is partially due to the fact that neXtSIM . . . the lead-fraction and heat-flux scaling and structure functions across different model resolutions.” - This paragraph is not clear to me. It is difficult to follow your line of argumentation. Please revise and rephrase.

The idea here is that if the opening-rate scalings are not resolution independent then we should expect the lead fraction (and heat flux) scalings also not to be resolution independent. We’ve modified the text to try to make this clearer.

P16, l320: “Conclusions” - You provide rather a summary of the paper than a conclusion. So, please change the title of the section accordingly.

We’ve changed this to “Summary and conclusions”

Data and code availability: A statement is missing, where to find the code and data of this study.

Done

Figure 1: “Lead fraction larger than 0.05 is indicated in yellow.” - Why do you show the thresholded fields instead of using a colormap that highlights the 0.05 fraction about shows the entire range of lead fractions? I recommend to use a show the entire range of lead fractions.

We now use a colormap that highlights the important range of lead fractions.

Figure 2: “The dashed straight lines are linear fits discussed in the text.” - Could you use color to indicate which fit belongs to which data. Please use different linestyle for the fits and the “Arctic”. Please also add all lines to the legend to clarify. In the caption “Arcitc” should be “Arctic”.

We've reworked this figure after not excluding the Beaufort Sea anymore, and in this case there's no need to differentiate between the two fits. We have added the all the lines to the legend.

Figure 4. Please add (a) and (b) labelling to the subfigures.

Done

Figure 7: "he" to "the". How do you choose the order of the polynomial fit of the structure functions here? For 12.5km and 25km the linear fit does not seem to be appropriate to fit the structure function, but rather a higher order (quadratic?) is required. This, however, would mean that the lead fraction gets multifractal for higher model resolution. Please elaborate on this difference when changing the model resolution in the text.

We've fixed the typo. We chose a linear fit for the structure function, same as in figure 3, and as you surmise. We chose this to be consistent with the analysis of the 6.5 km resolution run. Indeed the 25 km fit could be quadratic, but the uncertainty associated with the scaling at this resolution is so high that the significance of this is limited. This is now noted in the text.

References:

Wang, Q., Danilov, S., Jung, T., Kaleschke, L., and Wernecke, A.: Sea ice leads in the Arctic Ocean: Model assessment, interannual variability and trends, Geophys. Res. Lett., 43, 7019–7027, https://doi.org/10.1002/2016GL068696, 2016.

Hutter, N. and Losch, M.: Feature-based comparison of sea ice deformation in lead-permitting sea ice simulations, The Cryosphere, 14, 93–113, https://doi.org/10.5194/tc- 14-93-2020, 2020.

On the statistical properties of sea ice lead fraction and heat fluxes in the Arctic

Einar Ólason[1], Pierre Rampal[1,2], and Véronique Dansereau[1,3]

[1]Nansen Environmental Remote Sensing Center and Bjerknes Centre for Climate Research, Bergen, Norway
[2]Now at Université Grenoble Alpes, CNRS, Grenoble INP, Institut de Géophysique de l'Environnement, Grenoble, France
[3]Now at Université Grenoble Alpes, CNRS, Grenoble INP, Laboratoire 3SR, Grenoble, France

Correspondence: Einar Ólason (einar.olason@nersc.no)

Abstract. In this paper we explore several statistical properties of the observed and simulated Arctic sea-ice lead-fraction, as well as the statistics of simulated Arctic ocean-atmosphere heat fluxes. ~~We first~~ First we show that the ~~probability density function (PDF) and the~~ observed lead fraction in the Central Arctic has a monofractal spatial scaling, which we relate to the multifractal spatial scaling present in sea-ice deformation-rates. We then show that the relevant statistics of the observed lead fraction in the Central Arctic are both well represented by our model, neXtSIM. Given that the heat flux through leads may be up to two orders of magnitude larger than that through unbroken ice we then explore the statistical properties (PDF and spatial scaling) of the heat fluxes simulated by neXtSIM. We demonstrate that the modelled heat fluxes present a multifractal scaling in the Central Arctic, where heat fluxes through leads dominate the high-flux tail of the PDF. ~~In the Central~~ This multifractal character relates to the multi- and monofractal character of deformation rates and lead fraction. In the wider Arctic, the high-flux tail of the PDF is dominated by an exponential decay, which we attribute to the presence of coastal polynyas. Finally, we show that the scaling of simulated lead fraction and heat fluxes depend weakly on the model resolution and discuss the role sub-grid scale parameterisations of the ice heterogeneity may have in improving this result.

Copyright statement. The author's copyright for this publication is transferred to the Nansen Environmental Remote Sensing Center, Bergen, Norway.

1 Introduction

Sea ice is well known to be an excellent insulator. In the Arctic, it reduces the potential flux of heat from the ocean to the atmosphere by two orders of magnitude in the winter (e.g. Maykut, 1986; Andreas et al., 1979). Expanses of open water such as leads and polynyas on the other hand act to release substantial amounts of heat and moisture into the atmosphere, thereby promoting the production of new ice and the rejection of brine into the ocean. In particular, coastal and flaw polynyas produce large amounts of ice and their role in Arctic climate and oceanography has been widely studied ~~.~~ (e.g. Aagaard et al., 1981; Winsor and Björk, 2000; Morales Maqueda et al., 2004; Tamura and Ohshima, 2011). Leads in the centre of the Arctic Basin, on the other hand, are ~~a much more temporally and spatially clustered gateways for ocean–atmosphere~~

fluxesmuch more difficult to study because they are much narrower and shorter lived than polynyas, and at the same time can form anywhere in the Arctic Basin. However, processes surrounding lead formation are of considerable local importance and may have significant climatic influence as well, despite their extreme localisation (see for example Lüpkes et al., 2008a, b; Vihma et al., 2013, for an overview).

When a lead opens in the ice during winter, relatively warm ocean waters become exposed to the cold atmosphere, resulting in heat fluxes of up to 600 W/m^2 (Maykut, 1986; Andreas and Murphy, 1986). As a result, a plume of warm, moist air forms above the lead, sometimes resulting in ice fog, which significantly reduces visibility and can cause ice to accumulate on surfaces such as aircraft, power lines, and roads (Gultepe et al., 2015). This release of heat also causes drives convection in the predominantly stable or near-neutral Arctic atmospheric boundary layer (ABL) causing plumes of relatively warm and moist air to rise from the lead. In the presence of a capping inversion, the plume may penetrate the lowest levels of the inversion as it rises, leading to entrainment. Using data from an aircraft campaign, Tetzlaff et al. (2015) found that this kind of entrainment occurred in all four cases of capping inversion they studied, with entrainment fluxes reaching up to 30% of the surface heat fluxes. They also found clear evidence that this entrainment contributed significantly to warming the ABL downwind of the lead.

The transport of sensible heat flux, moreover, is significant over leads and was shown to be even more efficient over smaller than larger leads Andreas and Cash (1999); Esau (2007)(Andreas and Cash, 1999; Esau, 2007). Following up on the work of Andreas and Cash (1999), Marcq and Weiss (2012) estimated the lead fraction from a SPOT satellite image, covering 60×66 km^2. They demonstrated that, in that particular case, the sensible heat flux over the smaller leads could dominate that over the larger ones, such that including smaller leads increased by 55% the total estimated heat flux by 55%. This result points to a potentially significant under-representation misrepresentation of heat fluxes in large-scale atmospheric and coupled models, which neither resolve smaller leads nor accurately reproduce the properties of lead fraction statistics. Traditional sea-ice models are well known to only reproduce lead-fraction and linear-kinematic-feature properties when run at very high resolution and/or when care is taken that the momentum equation solver converges - and even then the model results are lacking in several aspects Girard et al. (2011); Wang et al. (2016); Spreen et al. (2017); Hutter et al. (2018). Neither of these requirements are met for the vast majority of model simulations used to study ice–ocean–atmosphere interactions in the Arctic, as the computational cost of doing so is substantial, although some progress is being made in this respect (Koldunov et al., 2019).

On the ocean side, the formation of new ice in leads removes fresh water and releases brine. Data from various field campaigns (e.g. Smith, 1974; Morison et al., 1992; Morison and McPhee, 1998), as well as numerical model results (e.g. Kozo, 1983; Smith and Morison, 1993; Smith et al., 2002) give a very consistent picture of brine release in leads. When the ice velocity is small or moderate, salt plumes form below the lead and sink to the bottom of the mixed layer. The plumes cannot penetrate the halocline but instead spread horizontally along the top of the halocline, reducing the depth of the mixed layer. When the ice velocity is sufficiently large, turbulent mixing occurs along the edges of the lead that distributes the rejected brine throughout the mixed layer. This process leads to large-scale convection in the mixed layer which deepens it and causes a vertically uniform salinity increase. Nguyen et al. (2009) showed that a faithful simulation of the Arctic halocline depends on

the proper simulation of brine release and its redistribution in the water column, while Barthélemy et al. (2015) demonstrated the importance of representing both the high- and low-velocity regimes when parameterising he brine release.

Leads, therefore, have a potentially significant role to play in the Arctic, through both their impact on the local weather conditions and their long-term influence on the state of the atmosphere and ocean. Even though their role in the ocean–atmosphere interaction is being actively researched (e.g. Esau, 2007; Lüpkes et al., 2008a, b; Marcq and Weiss, 2012; Chechin et al., 2019; Li et al., 2020, and the mechanisms of lead formation are well known, the statistical properties of leads in large-scale sea-ice models have not yet been shown to be robustly reproduced. ~~Lead formation is closely linked to the temporal and spatial localisation of sea ice deformation~~When sea ice deforms ridges and leads form. Consequently, the probability distribution functions (PDF) of open water densities, floe sizes, and deformation rates share the common property of a "heavy tail" (Rothrock and Thorndike, 1984; Matsushita, 1985; Stern et al., 2018; Weiss, 2003; Marsan et al., 2004; Marcq and Weiss, 2012) that is a sign of scale-invariance. Deformation rates (Marsan et al., 2004; Hutchings et al., 2011; Bouillon and Rampal, 2015a; Rampal et al., 2019) and open water densities (Weiss and Marsan, 2004) have been shown to display multifractality in the space domain and, in the case of deformation rates, in the time domain also (Weiss and Dansereau, 2017; Rampal et al., 2019). ~~This fundamental property is the signature of both spatial localisation, as well as of spatial localisation that is more pronounced for large deformation events.~~

The fractal characteristics of deformation rates and other quantities are of particular interest because their presence may give us interesting information about the underlying mechanisms at play in the physical system. In the case of deformation of geophysical solids as sea ice a fractal characteristic comes about, at least in part, because of a propagation of fracturing events, which can be modelled by multiplicative cascades (Weiss and Marsan, 2004). Fracturing triggers a redistribution of stresses in the ice, which in turn trigger more deformation nearby. Large deformation events are also likely to be recurrent where previous fracturing has already weakened the ice, resulting in a multi-fractal character (Weiss and Marsan, 2004; Marsan and Weiss, 2010). A well known analogue is crustal deformation, where earthquakes cause a redistribution of stresses in the earth's crust, with large quakes clustered around weak areas in the crust and smaller quakes more distributed in the vicinity (Kagan, 1991). In this study, we ~~compare the properties of lead fraction statistics calculated from passive microwave satellite data to that simulated by a continuum sea icemodel. The model used, neXtSIM, is the first modelthat was shown to reproduce the observed multifractality of sea ice deformation rates in both space and time (Rampal et al., 2019)~~investigate how the fractal character of sea-ice deformation (see Bouillon and Rampal, 2015a; Rampal et al., 2016, 2019) affects lead fraction and heat fluxes through the ice, using observations and the neXtSIM model.

~~Section 2.1 presents~~

In Section 2 we present briefly the model setup, as well as the data and the methodology of the scaling analysis performed in this study. ~~Section 3 demonstrates that~~ In section 3 we present the probability density function (PDF) and spatial scaling of ~~lead fraction~~ the observed lead fraction. We also demonstrate that the PDF and spatial scaling simulated with neXtSIM match ~~very~~ well with those observed~~by satellite remote sensing~~. The capability of the model to reproduce lead fraction statistics justifies its use in further analysing atmospheric heat flux statistics and inferring the role of leads in determining the properties of these statistics ~~. This —~~ which is done in section 4. ~~A brief investigation of~~ Following this we briefly investigate the influence of model resolution on our results ~~is presented~~ in section 5~~, where~~ . There we show that the lead-fraction scaling and the heat-flux

scaling depends only weakly on the model resolution. ~~Section 6 touches upon~~ In section 6 we then discuss the model evaluation against observations and the ~~on the~~ origin of the shape of the PDF of heat fluxes and their spatial scaling, for both the so-called "Central Arctic" (i.e. excluding coastal areas) and the whole Arctic basin. We also discuss the source of the multifractal scaling for the heat fluxes and the role of surface heterogeneity in the localisation of heat fluxes at different model resolutions.

2 Model, data, and methodology

2.1 Model set-up

We use the latest version of the next generation sea ice model, neXtSIM, presented in Rampal et al. (2019). NeXtSIM is a stand-alone sea-ice model, coupled to a slab ocean and forced by the results of atmospheric and oceanic reanalyses. It uses the Maxwell-Elasto-Brittle (MEB) rheology of Dansereau et al. (2016), a Lagrangian moving mesh as described in Rampal et al. (2016) and the two-layers thermodynamics model of Winton (2000). Heat fluxes between the ocean, ice, and atmosphere are calculated using traditional bulk formulae, as outlined by Rampal et al. (2016). Oceanic heat loss results in lowering of the slab ocean temperature, which may be compensated for by new-ice formation and nudging of the slab ocean layer temperature to reanalysis results. The model has in essence three ice categories: those of thick ice, open water, and a category of newly formed thin ice. The ice thickness redistribution and thermodynamic schemes are outlined in the appendix of Rampal et al. (2019). All output variables are interpolated using a conservative scheme from the moving Lagrangian model mesh onto a fixed and regular Eulerian grid and are averaged on a daily basis to match the temporal resolution of the observations (see Section 2.2).

The model set-up covers the central Arctic Ocean, with open boundaries at the Bering Strait, the Canadian Arctic Archipelago, Greenland, and the Barents and Kara Seas (see figure 1). The model's triangular mesh is built on the 6.25 km resolution grid of the lead fraction data set (Ivanova et al., 2016, see section 3) such that the two have the same coast lines and comparible resolutions. This is done to simplify the comparison of the two. In all other respects the model setup is the same as that of Rampal et al. (2019): it is forced using the ocean state from the TOPAZ4 oceanic reanalysis (Sakov et al., 2012) and the atmospheric state of the Arctic System Reanalysis[1] (Bromwich et al., 2016). The model is initialised with sea ice concentration and thickness from ~~a combination of the TOPAZ4 reanalysis, and the~~ the OSISAF climate data record (Tonboe et al., 2016) and ICESAT[2] ~~Kwok et al. (2009)~~ (Kwok et al., 2009) datasets respectively. We use resuts from the TOPAZ4 reanalysis to fill in gaps in the ICESAT thickness. The initial snow thickness is set based on the Warren et al. (1999) climatology and ice age, using half the climatological snow thickness over first year ice. We start the model on November 15th, 2006, restricting our analysis to the winter months of January, February and March (JFM), 2007, during which the Arctic Ocean is fully ice-covered, and ice growth is high; hence the mechanical and thermodynamical regimes are approximately uniform.

We run three simulations, in addition to the control simulation, covering the same space domain and time period. The forcings are the same in the three cases. Two of these simulations investigate the effect of changing the model spatial resolution, and

[1]https://rda.ucar.edu/datasets/ds631.0, ASRv1 30-km, formerly ASR final version, Byrd Polar Research Centre/The Ohio State University. Accessed 15 April 2015

[2]https://icdc.cen.uni-hamburg.de/1/daten/cryosphere/seaicethickness-satobs-arc.html

one investigates the effect of changing the model's rheological framework. We run the simulations related to model resolution at ~~10 and 20 km node spacing~~12.5 and 25 km resolution, with all model parameters kept the same as in the control run. An exception to this is the cohesion, c, as this parameter scales with the model resolution as

$$c \sim 1/\sqrt{L_m},$$

where L_m is the model resolution ~~(as is done in Bouillon and Rampal, 2015a)~~(see Bouillon and Rampal, 2015a, for further de
.

In the third simulation, the MEB rheology is replaced with a linear viscous rheology. The deficiencies of the linear viscous model are well known, and it is neither suited for a detailed study of the model physics nor model evaluation (see e.g. Leppäranta, 2005, and
. It is used here to investigate, in a simple and straightforward manner, the effect of not simulating highly localised leads in the Arctic, while at the same time simulating some polynya formation. As the solution of the linear viscous model quickly degrades we initialise the model with smoothed model results from the control run at weekly intervals, giving the model three days to spin up after each initialisation. This way the model solution has some time to evolve after initialisation, but not enough time to degrade significantly. The value we use for the viscosity parameter coincides with the lower bound suggested by Hibler (1979) ($\zeta = 1.0 \times 10^{10}$ kg/s), as this gives a reasonably good drift speed compared to the OSI-SAF drift product, in our set-up. We did not attempt to tune the viscosity value further, as this model run proved sufficiently adjusted for the purposes of this study.

2.2 Observational data

We ~~evaluate the modelled lead fraction against~~ analyse observed lead fraction from Ivanova et al. (2016), ~~which is an improvement~~ as well as using it to evaluate the model results. This product improves on the original product from Bröhan and Kaleschke (2014) by correcting an overestimation of the lead fraction by a simple adjustment of the upper tie point used in the method. This product is based on passive microwave observations of the AMSR-E and is a daily, light and cloud independent, pan-Arctic data set, available from November to April, for the period 2002–2011. The dataset resolution is 6.25 km and the method allows the detection of leads wider than 3 km, meaning that a substantial amount of smaller leads are undetected in this product.

The data shows the area fraction of each grid cell that is covered by leads filled with open water, thin ice, or a mixture thereof. The observations are filtered for feature orientation and the product, therefore, shows only the fraction of leads, excluding larger, non-linear features such as seasonally thin ice and polynyas. Although the thickness threshold for thin-ice detection in this product is not known precisely, it is unlikely that this approach classifies ice thicker than about 10 cm as thin ice (Röhrs and Kaleschke, 2012).

2.3 Methodology

We briefly outline the methodology for investigating the statistical properties of lead fraction and heat fluxes here. More details can be found in Schertzer and Lovejoy (1987), Marsan et al. (2004), and Rampal et al. (2019). The first step in characterising the statistics of a process that exhibits scale-invariance is to consider the PDF of its realisations or event magnitudes. If the

PDF has a tail that ~~follows a power law (i.e. a straight line on a log-log plot~~is "fat" (e.g. a power law, stretched exponential, log-normal), there is potentially a fractal spatial scaling to be found for the quantity. The slope of such a tail indicates the extent to which extreme events dominate the process studied and which moment ~~order is~~ orders are required to properly describe the distribution of event magnitudes. The PDFs shown in this paper combine all ~~values available~~ the daily means for JFM, ~~2011, i.e. all daily means for~~ 2007 for both the lead fraction and ~~all snapshots for the~~ heat flux magnitudes (see figures 2 and 4).

The second step is to investigate changes in the PDF of both the lead fraction and heat flux magnitudes (hereafter referred to as heat fluxes) with respect to the scale of observation. In this study, we focus on the space domain and, therefore, set the temporal scale of analysis. We choose the daily time scale to consistently compare simulated and observed lead fraction, and we retain the daily time scale for the sake of simplicity when analysing the heat fluxes. The scaling analysis consists of evaluating the different moments of the distribution at different spatial scales. The moments of the distribution are calculated as

$$\mu_q = \frac{1}{N}\sum_{j=1}^{N} x_j^q, \tag{1}$$

where q is the moment order, N is the number of samples, and x_j are individual samples.

In the coarse-graining analysis, the mean and higher-order moments are calculated at varying spatial scales, L, by averaging the observed and simulated values onto incrementally coarser grids. In order to calculate the mean scaling for JFM, we calculate the scaling for each daily mean or snapshot and take the temporal mean of the means and moments calculated at each spatial scale. In the Eulerian case, the coarse-graining grid is set by the averaging grid, while in the Lagrangian case the coarse-graining grid can be chosen arbitrarily. In the Lagrangian case, we follow Marsan et al. (2004) and combine the results of differently placed coarse-graining grids at each spatial scale to improve the robustness of our statistics. For spatial scales larger than that of the observations or model, each cell of the coarse-graining grid may consist of a large number of land points (in the Eulerian/lead-fraction case) or few model elements (in the Lagrangian/heat-flux case). In the Eulerian case, we therefore assume that if the number of land points is more than half the points in a cell of the coarse-graining grid the data in that cell is not reliable and we discard it. In the Lagrangian case, we discard data if the number of model elements in a coarse-graining cell is less than half the median number of elements in all the cells.

Using the spatial coarse-graining method we produce plots of the moment values as a function of the scale ~~of observation~~ (see figure 3 and figure 5). When presented in the log-log space, the moment values should decrease linearly with increasing L. The slope of this linear decrease, β, is estimated for each moment order, q. The slope expresses a spatial scaling such that the moments are $\mu_q \sim L^{\beta(q)}$ and ~~$\bar{x} \sim L^{-\beta(0)}$~~ the mean is $\bar{x} \sim L^{-\beta(1)}$, where L is the spatial scale. ~~It is important to note that we calculate the slopes of the scaling using logarithmically-spaced L bins and by applying a least squared method to the binned data, in the log-log space. Stern et al. (2018) argue that this method provides a reasonably accurate estimate of the power-law fit. We , however, keep in mind that their alternative method based on a Maximum Likelihood Estimate might provide an even more accurate estimate and plan its implementation for future works.~~

~~Finally, we~~ We then calculate the structure function, $\beta(q)$, which describes the change in the slope of the scaling as a function of the moment order. We estimate the uncertainty relative to this calculation as the 95% confidence interval of a least-squares linear fit of the $(L, \bar{x}(L))$ and $(L, \mu_q(L))$ points.

For a quantity ~~that scales~~related to a so-called scale invariant process, there is generally a monotonic change in β with increasing q. The scaling is monofractal if $\beta(q)$ is linear and multifractal if $\beta(q)$ is parabolic. If the scaling is monofractal only the spatial organisation ~~is linked to a fractal~~ of the quantity is following a fractal pattern, with no ~~link to the~~ dependence to the actual magnitude. If it is multifractal, however, the ~~highest~~ higher values are also ~~linked to a fractal~~ distributed following a fractal pattern and thus are more localised than lower values.

3 Model evaluation against observed lead fraction

In this section, we demonstrate the capability of neXtSIM to reproduce lead-fraction statistics by comparing the statistical properties of simulated and observed lead fractions. As the observed lead fraction corresponds to the fraction of open water as well as thin ice (Röhrs and Kaleschke, 2012), we define the simulated lead fraction for the purpose of this comparison as the sum of the simulated open water fraction and of the fraction of new ice that is thinner than a given threshold. The correct threshold for thin ice is not well constrained since the maximum ice thickness that is classified as a lead in the satellite data is not well defined either. We, therefore, choose a threshold thickness for the model that ~~gives good statistics and, in particular,~~ the same slope of the PDF as the observed one, as shown below. For the JFM average, this optimal threshold is ~~9.1~~9.8 cm, but variations of this value by about 1 cm still give good agreement with the observations. This value is reasonable, given that Röhrs and Kaleschke (2012) estimates an upper bound on thin ice at 10 cm in their product.

It is important to note that the simulated lead fraction is not strictly a lead fraction as it includes all open water areas, including polynyas (cf figure 1). In contrast, the observed lead fraction data is filtered so that polynyas are left out of the final product. To allow for a fair comparison of the simulated and observed lead fraction, we therefore define a polynya-free region referred to here as the "Central Arctic", which covers the area more than 400 km northward of the 20 m isobath (see figure 1).

Figure 2 shows the PDF of observed and simulated lead fraction on a log-log scale. The observed and simulated PDF shows a linear decrease for lead fraction larger than about 40%, as expected based on the work of Marcq and Weiss (2012). ~~For the observations, however, the linear relationship is not as clear, showing a deviation from linearity at around 70% (figure 2, dashed blue line). The source of this deviation is in the Beaufort Sea. When excluding this region, the observations also show a linear decrease (Fig. 2, solid blue line). The~~ The slopes of the PDF for the observed and modelled lead fraction are then very similar. The choice of thin ice threshold for the model is based on matching these slopes (~~−4.3~~−3.9) over the lead fraction range of $[0.40, 0.93]$. ~~The reason why including the Beaufort Sea destroys the linear trend in the tail of the PDF for the observations is not clear. However, we suspect that the large number of small leads forming there may result in increased noise in the lead fraction product (see Fig.1) and an overestimation of the large lead fractions.~~

For values smaller than about 40%, the PDF for the observations flattens out. This behaviour is to be expected as the small leads are known not to be captured by the AMSR-E because of its resolution limitation and, therefore, are not present in this

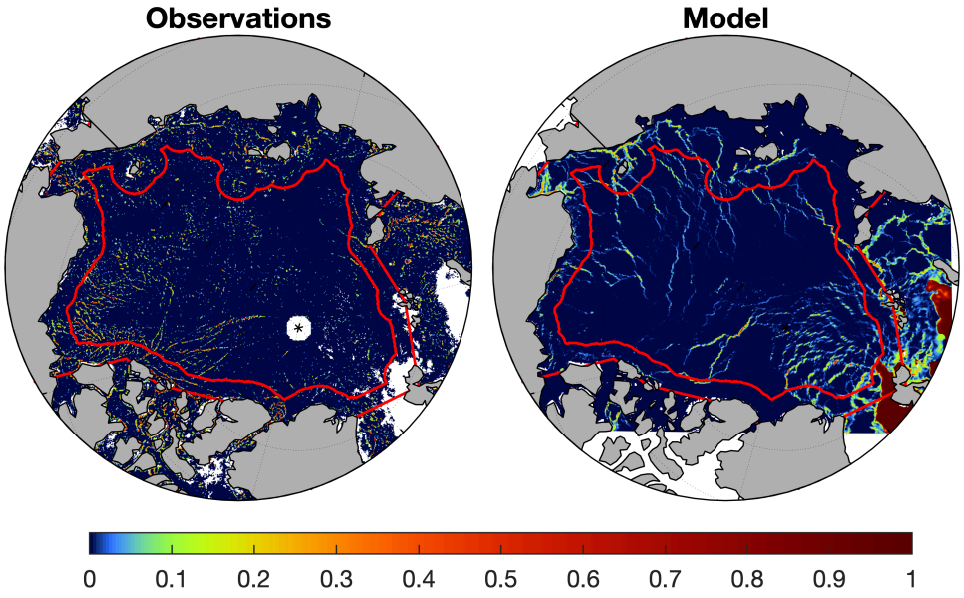

Figure 1. Observed and simulated ~~active leads~~ daily mean lead fraction on ~~January 1st~~March 14th, ~~2011.~~ 2007. The figure shows the entire model domain, and the ~~read~~ red lines indicate the boundaries of the "Arctic" (outer region) and "Central Arctic" regions used in the study. ~~Lead fraction larger than 0.05 is indicated in yellow.~~ Note the presence of polynyas in the model output and the presence of noise in the observations.

product. It is worth noting that although the spatial resolution of the model is similar to the resolution of the satellite product, the model can capture smaller leads, demonstrated by the absence of flattening of the PDF for small values. The slope of the simulated PDF does change at smaller values, becoming linear again below 2% (not shown).

We now consider the spatial scaling of the lead fraction for the first four moments of the distribution, as the absolute value of the slope of the PDF in the lead fraction range of $[0.40, 0.93]$ lies between 4 and 5 (Marsan et al., 2004). The spatial scaling, along with the resulting structure function, is given in figure 3 and shows ~~an excellent~~ a good agreement between the model and observations. The mean is conserved across scales, as expected, but the mean lead fraction is higher in the model than the observations. This discrepancy appears because small values of the lead fraction are under-represented in the observations. The mean observed and simulated lead fractions are ~~0.0034 and 0.0044~~0.0055 and 0.0047. However, the means of the observed and simulated lead fractions larger than ~~20% are 0.313 and 0.315~~ 40% are 0.554 and 0.552 respectively. The higher order moments of the observed and simulated lead fractions are in good agreement for all lead fraction values, but are virtually identical if we consider only lead fractions larger than ~~20%.~~ 40%. This shows that the agreement between model and reality is probably much

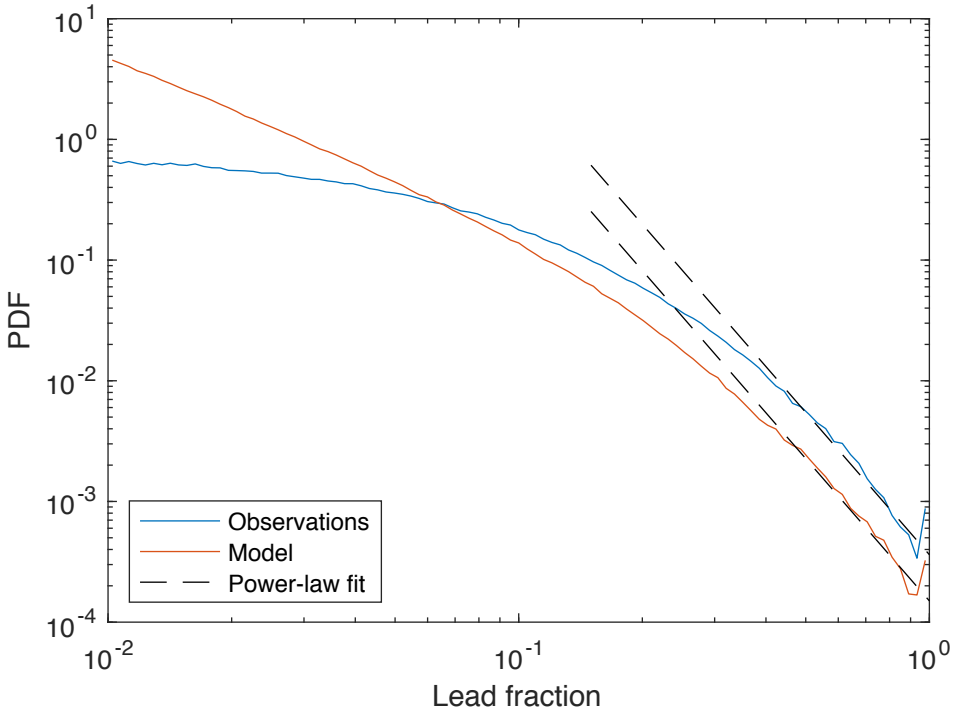

Figure 2. The probability density function of observed and simulated lead fraction in the "~~Arcitc" (dashed) and "~~Central ~~Arctic~~Arcitic" ~~(solid)~~ areas over JFM ~~2011.~~ 2007. The dashed ~~straight~~ black lines are linear fits discussed in the text.

better than a first-order interpretation of figure 3 would suggest. Perhaps a fairer comparison between the model simulation and observations would therefore consider only lead fractions larger than ~~20~~40%. However~~it~~, that would greatly complicate the spatial scaling calculations.

The structure function underlines the good agreement between the simulation and observations: within the estimated uncertainties, the slopes of the observed and simulated structure functions are ~~0.9 ± 0.1 and 0.8 ± 0.1 respectively~~ 0.650 ± 0.006 and 0.78 ± 0.06 respectively using a least-squares fit (see figure 3). We note that this structure function is linear and therefore that the scaling is monofractal. The good agreement between the observed and modelled structure function, together with the good agreement between observed and modelled mean and higher order moments accounting for only lead fractions larger than ~~20%~~ 40% (see above) is a strong indicator that the model is simulating ~~realistic lead-fraction patterns~~ lead formation in a physical and realistic manner — even if the incompleteness of the observations does not allow a closer comparison than that done here.

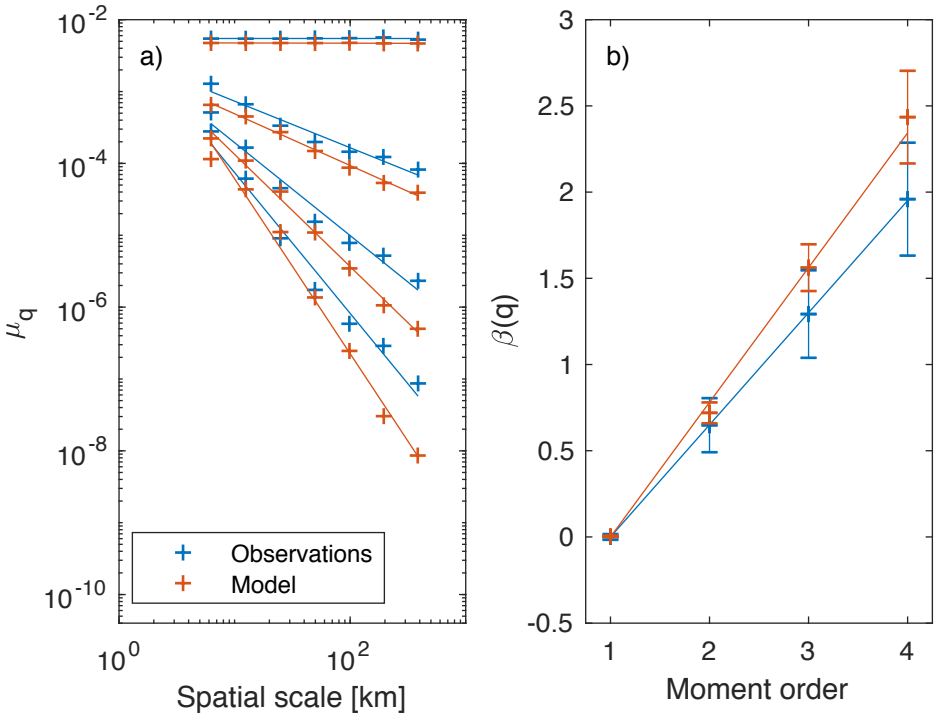

Figure 3. Left pane: The spatial scaling of observed and simulated lead fraction in the "Central Arctic" region over JFM ~~2011.~~ 2007. The lines are ~~power law~~ fits for each moment (order 1, 2, 3, and 4 from top to bottom). Right pane: The resulting structure function for both observed and simulated lead fraction. The lines are linear fits.

4 Modelled heat fluxes

We now explore the statistical properties of the heat fluxes simulated by neXtSIM. Figure 4 shows the PDF of simulated heat fluxes for both the "Arctic" and "Central Arctic" regions. When plotted on a log-log scale the PDF shows a clear linear tail for heat flux values between 30 W/m^2 and 110 W/m^2, with a slope of -3.4, within the Central Arctic region (figure 4a), dropping off rapidly for larger flux values. In the Arctic region, however, the tail is not linear on the log-log plot, but it is linear on a semi-log plot for heat flux values larger than 200 W/m^2 (figure 4b). We, therefore, expect to see ~~proper~~ spatial scaling only within the Central Arctic region. We note that the exponential decay displayed in the Arctic region is most likely related to the large coastal and flaw polynyas impacting the heat fluxes there.

Given the results of the analysis of the PDF, we consider the first three moments for the spatial scaling of heat fluxes, confining the analysis to the Central Arctic region. The results of this analysis are plotted in figure 5, which shows a clear scaling of the heat fluxes in space. Although there is substantially more scatter in this plot than in the lead fraction analysis (figure 3) it still clearly indicates that the scaling is multifractal.

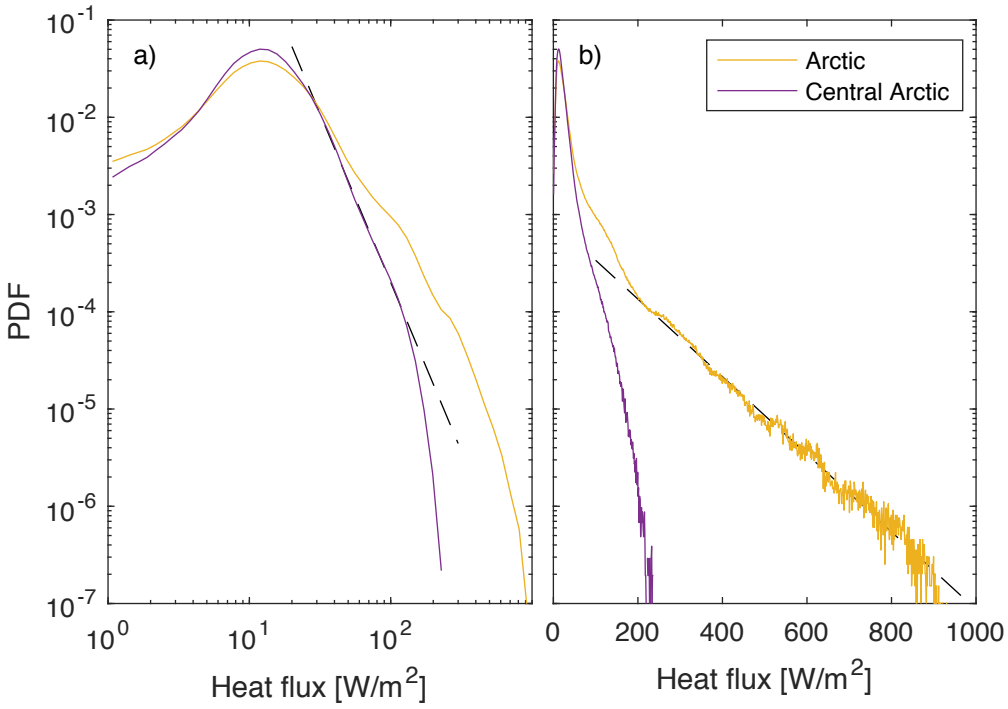

Figure 4. The probability density function of modelled atmospheric heat flux in the "Arctic" and "Central Arctic" regions over JFM. The dashed lines are linear fits discussed in the text.

To demonstrate the role of leads in the scaling obtained for the simulated heat fluxes we ran the model with a linear viscous rheology, as described in section 2.1. In this case, no leads form in the Central Arctic, but coastal and flaw polynyas do form. The PDF of the heat fluxes simulated with the viscous model over JFM 2007 is shown in figure 6. This experiment demonstrates that when using the linear viscous model, the tails of the distribution are significantly reduced in the Central Arctic region, so much so that one should suspect the absence of spatial scaling there. A spatial scaling analysis region indeed confirms that both the mean and the higher moments are the same at all spatial scales (not shown), as expected for a homogeneous fluid.

In the Arctic region we still obtain an exponential decay with the viscous model. This result supports the idea that this exponential function is the expression of the presence of polynyas in that region, since polynyas are present in both the MEB and viscous simulations.

5 Effects of resolution

To briefly explore the effects of the model resolution on the statistics of simulated lead fraction and heat fluxes we ran the model in the same configuration, but at 12.5 km and 25 km resolution (see section 2.1). The results of the scaling analysis for all three model resolutions are shown in figure 7 for the lead fraction and figure 8 for the heat flux. The comparison shows that

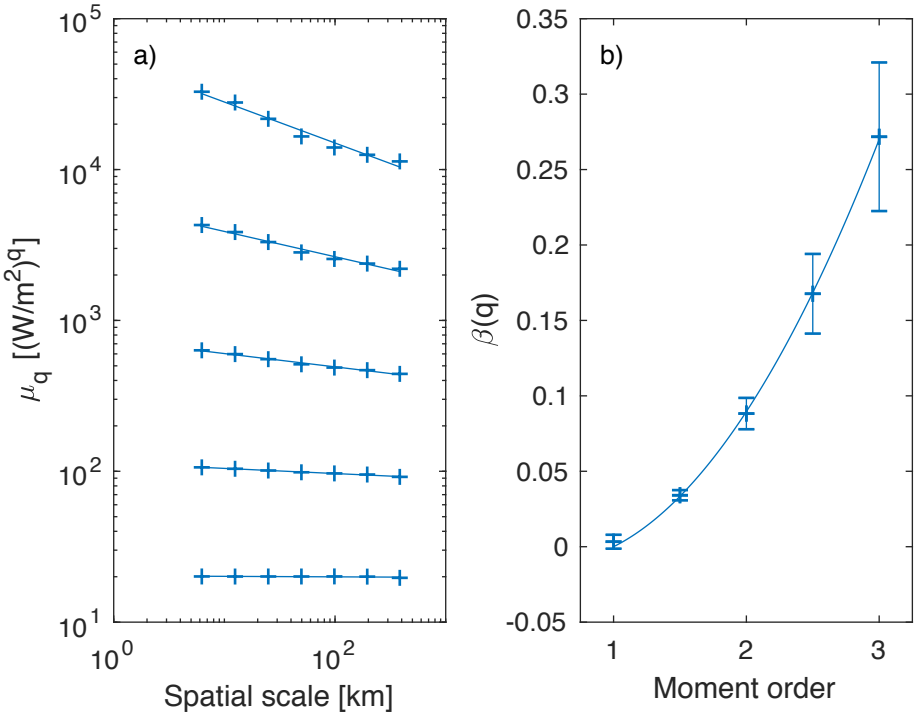

Figure 5. Left pane: The spatial scaling of simulated heat fluxes in the "Central Arctic" region over JFM ~~2011.~~ 2007. The lines are ~~power law~~ fits for each moment (order 1, 1.5, 2, 2.5, and 3 from bottom to topp). Right pane: The resulting structure function. The lines are linear and quadratic fits.

the simulated lead-fraction scaling depends on model resolution, as all three model runs give different mean and higher order moments, and structure function. The difference in the mean between different resolutions is small, 30% between the 6.25 and 12.5 km resolution runs and 20% between the 12.5 and 25 km resolution runs, while higher order moments see increasing differences towards smaller spatial scales.

This result means that running the model at different resolutions will give nearly the same values for the mean, while for the higher order moments model runs at different resolutions will give different values. The difference between the runs at 6.25 and 12.5 km resolution are only modest, while going to 25 km resolution results in significant differences for the third and fourth moments~~.~~, with a much less cleaner scaling as well. These differences also result in a change in the structure function, which could be multifractal, rather than monofractal for the 25 km resolution. The significance of this is limited by the large uncertainties associated with the scaling at 25 km resolution.

For the simulated heat fluxes there are similarities but also clear differences between the results of simulations at different model resolutions. The mean heat flux is nearly the same for all simulations and conserved at all scales. All three models also show a clear scaling of the higher order moments and very similar statistics at the lowest spatial scales. The main difference

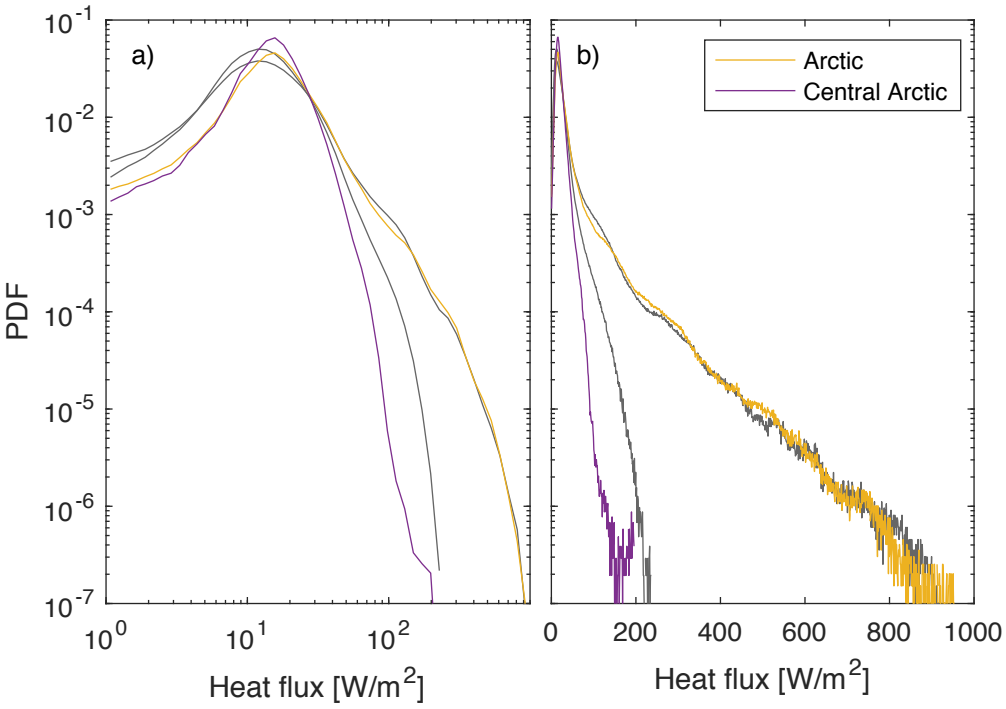

Figure 6. The probability density functions of modelled atmospheric heat flux in the "Arctic" and "Central Arctic" regions over JFM, using the viscous (coloured lines) and MEB (grey lines) rheological models.

between the different model results is that, at small spatial scales, higher model resolution gives higher values for the higher order moments. The slopes of the scaling and, therefore, the values of the structure function, are thus higher for the higher resolution runs.

In addition to these differences in the scaling, there also seems to be a difference in the nature of the structure function, depending on the model resolution. The structure function at 6.25 km resolution clearly indicates a multifractal scaling. This is also the case at 12.5 km model resolution, even though the uncertainty is higher and the structure function is smaller. Going from the 12.5 km to the 25 km model resolution continues the shift in the structure function going from 6.25 km to 12.5 km, of decreasing slopes and increasing uncertainty. As a result, we cannot say with any confidence that the structure function indicates a multifractal scaling at the 25 km resolution. This change mirrors the change in fractality for the lead fraction going to 25 km from 12 km resolution.

6 Discussion

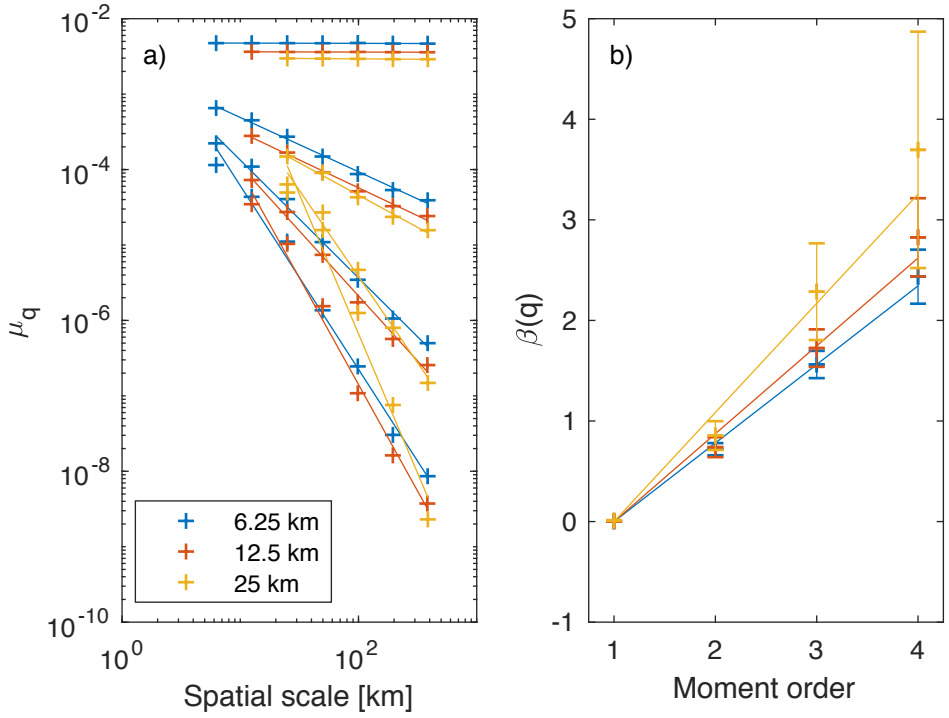

Figure 7. The spatial scaling and structure function of modelled lead fraction in the "Central Arctic" region over JFM, ~~2011.~~ 2007. The two panes are the same as figure 3, only here ~~he~~ the colours denote results from runs at different model resolutions.

We have shown that the observed and modelled lead-fraction statistics in the Arctic have a monofractal character, as revealed by a spatial scaling analysis. This fractal character is inherited from the multifractal character of the ice deformation rates, as discussed below. The fact that the lead-fraction statistics are fractal means that the event propagation mechanism that generates fractal deformation rates also generates fractal lead fraction - which is to be expected. We note that the lead fraction has a monofractal character, while the deformation rates are multifractal. This means that while large deformations are more localised than small ones, all leads are localised equally. We did not investigate the difference especially, but a likely explanation is that the lead fraction has too little variation to give multifractal statistics - it is essentially in either an on or off state. The modelled heat fluxes, on the other hand, do show a multifractal scaling, and this is probably because the heat flux is much more sensitive to the thickness of newly formed ice then the lead fraction.

We have compared the fraction of pixel area covered with open water or thin ice within a lead as estimated from passive microwave satellite data to the modelled fraction of open water and newly formed ice thinner than ~~9.1~~ 9.8 cm in neXtSIM. Our analysis shows that the agreement between the two is very good, and improves when we take into account the fact that small leads are under-represented in the observations. This under-representation of small leads is most likely the largest source of uncertainty in the present comparison. It is not clear whether the model needs further tuning or enhancement at this point.

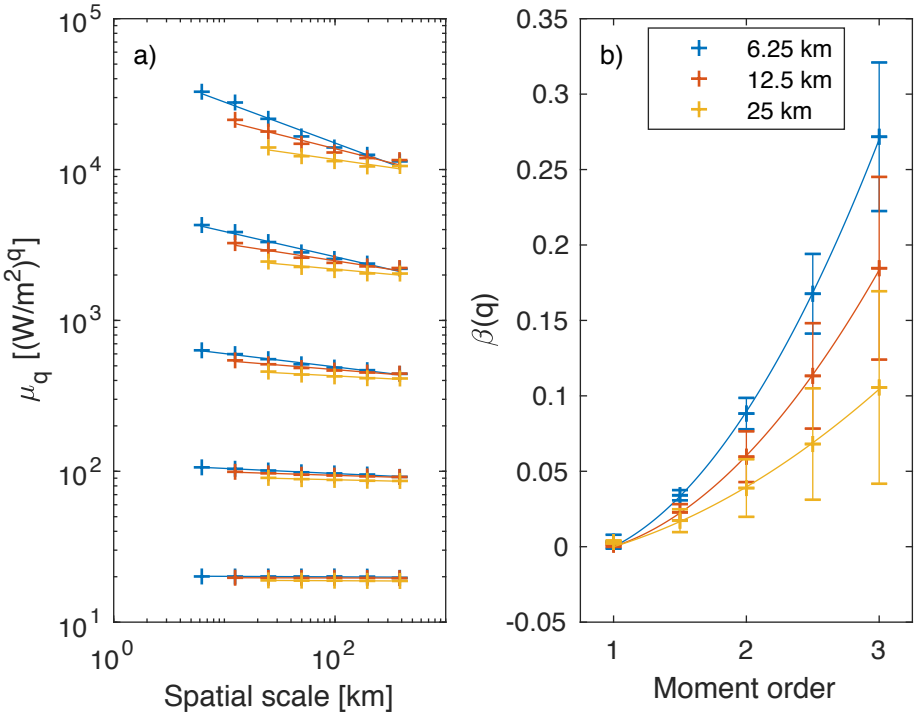

Figure 8. The spatial scaling of modelled heat fluxes in the "Central Arctic" region over JFM, ~~2011.~~ 2007. The two panes are the same as figure 5, only here he colours denote results from runs at different model resolutions.

The next step would be to compare neXtSIM with other lead fraction datasets at higher resolution, e.g. from Synthetic Aperture Radar (SAR) images or the Moderate Resolution Imaging Spectroradiometer (MODIS, see Willmes and Heinemann (2015)). Such comparison is however considered to be outside the scope of the present paper. Our conclusion from our model evaluation is that the statistics of simulated lead fraction are well enough represented in neXtSIM to allow analysing the effects of lead opening on the heat fluxes using this model.

Considering the PDF of simulated heat fluxes, we note that we obtained a linear tail on a log-log scale in the Central Arctic region and a linear tail on a semi-log scale in the Arctic region. Using the results of the viscous model simulations, we showed that the log-log tail in the Central Arctic disappears when no leads are present, while much of the semi-log tail in the Arctic region remains. This suggests that the log-log tail in the Central Arctic and the observed scaling of heat fluxes is directly related to the formation of leads there. The semi-log tail in the Arctic can then be related to polynya formation, which does occur in the viscous model.

To explain how polynya formation causes the semi-log tail in the Arctic we use a simple model of ice growth in a polynya. This model assumes the polynya to be instantaneously opened by the wind and then closed due to ice growth ~~. We also~~ where all ice that forms inside the polynya is herded by the wind to its down-wind edge. We can then assume that the closing rate is

directly proportional to the area of the polynya since ~~most of the~~ the total heat loss and ~~ice formation happens over~~ total ice formation can be assumed to be proportional to the area of open water. An equation for the area evolution of the polynya is then

$$-\frac{dA}{dt} \propto A, \tag{2}$$

where t denotes time and A the polynya area. The solution to this ordinary differential equation is

$$A = A_0 e^{-tC}, \tag{3}$$

where A_0 is the initial polynya area, and C is the growth rate of ice in the polynya. Letting A evolve over time, we can see that the resulting PDF, P, has an exponentially decaying tail. Since the PDF is the normalised derivative of the cumulative distribution function, which is, in turn, an integral of A from 0 to ∞, we have ~~after some algebra~~

$$P(x) = Ce^{-xC}. \tag{4}$$

Since we can assume the heat flux is proportional to the polynya area, to first order, we can expect the PDF of the heat flux to follow the same basic behaviour.

The linear tail on a log-log plot observed in the Central Arctic in figure 4a does not extend to the very highest simulated heat flux, as we would maybe expect. The reason for this discrepancy was not identified, but two likely explanations can be readily put forth. On the one hand, this effect could be physical; the largest fluxes produce ice the quickest, and hence we could expect this rapid ice growth to quickly dampen the heat flux and destroy the linear relationship. On the other hand, this could be a model artefact; we can imagine the sub-grid scale heterogeneity of newly formed ice to play a larger role for large heat fluxes than for small ones, and we know this heterogeneity to be only crudely parameterised in the model. Determining which of these explanations is true, and understanding their physical impact, is non-trivial and will not be attempted here.

Having analysed the PDF of heat fluxes for both the Arctic and Central Arctic regions we focused on the Central Arctic, where we found a clear multifractal scaling of the simulated heat flux. It is interesting that the heat-flux scaling is multifractal while the lead-fraction scaling is monofractal. This difference shows that, in the case of heat fluxes, the high values are also more localised in space, as is the case for sea-ice deformation (Marsan et al., 2004; Rampal et al., 2008; Stern and Lindsay, 2009; Bouillon and Rampal, 2015b; Rampal et al., 2019). This behaviour is to be expected, to some extent, because the largest heat fluxes depend not only on the lead fraction but also on the fraction and thickness of the newly formed ice in the leads. There is, therefore, additional information that goes into the heat-flux calculation, compared to the lead-fraction calculation, giving the potential for a multifractal scaling.

The current model does not take lead width into account when calculating the heat flux, as suggested by Andreas and Cash (1999). If it did, we would expect even stronger multifractality, as the highest heat fluxes would be even more localised. With the current approach, however, the presence of multifractality indicates the importance of properly localising the heat fluxes, since it is at these locations that the largest heat fluxes also occur. The best platform to investigate these effects is, of course, a coupled ice–atmosphere model, where the localisation of heat fluxes can influence the atmosphere in a manner similar to

what Esau (2007) and Marcq and Weiss (2012) have started exploring. Coupling the ice with an ocean model is likely to have smaller effect in at the time scales we consider here. Over a single winter the slab ocean model should be a sufficient simulation of the heat reservoir delivered by the ocean surface mixed layer. At longer timescales though, a coupling with the ocean likely becomes necessary to represent the evolution of the mixed layer and halocline.

We also briefly explored the impact of model resolution on the simulated lead fraction and heat fluxes and found that the statistics of the simulated lead fraction and heat fluxes are affected by the model resolution. This ~~is partiallydue~~ can, at least partially, be traced to the fact that neXtSIM does not exactly preserve deformation-rate ~~scalings~~ (and in particular the opening-rate) scaling for the second and third moments and the structure function across different model resolutions (see figure 12 of Rampal et al., 2019). We can ~~, therefore, not~~ assume that the model's ability to reproduce the observed lead-fraction is due to its ability to reproduce the observed opening rates. Thus, if the scaling of the modelled opening-rates are not preserved across different model resolutions then we should expect the resulting ~~opening rates, lead fraction , and heat fluxes to preserve those statistical properties~~lead fraction and heat flux scaling also not to be preserved. However, considering that the model does conserve the scaling for the first moment (the mean) of the deformation rates (see figure 12a of Rampal et al., 2019)) across different resolutions but not that of the lead fraction and heat fluxes, it is also likely that a lack of sub-grid scale heterogeneity of the ice thickness distribution in the model plays an important part in its inability to preserve the lead-fraction and heat-flux scaling and structure functions across different model resolutions.

The sub-grid scale thickness distribution used in neXtSIM is a very crude approximation of the highly heterogeneous thickness distribution present in reality. Furthermore, running the model at a high resolution should capture heterogeneity of the ice that should otherwise be parameterised in a coarse resolution model. As such, even if the deformation scaling were preserved across different model resolutions, one would not necessarily expect the lead-fraction or heat-flux scaling to be preserved. Realistically, the only way to achieve this would be to use a much better parameterisation of the sub-grid scale thickness distribution.

The main implications of ~~this~~ these model shortcomings can be expected to be related to the influence an underestimation of the higher order moments of the heat fluxes has on the atmosphere and ocean in a coupled setup. It means that while different model resolutions will deliver the same mean heat fluxes and the same heat-flux statistics on the largest scales, we can expect extreme events to be underestimated in a coarse resolution model. This in turn may lead to an underestimation of local effects, such as mixing, moisture transport, and brine release — the large scale impact of which cannot be estimated here.

7 Conclusions

Summary and conclusions

In this paper, we have evaluated the simulated lead fraction in neXtSIM against observed lead fraction using scaling analysis. We then investigated the scaling of heat fluxes in neXtSIM and the conservation of lead-fraction and heat-flux scaling across different model resolutions. The main results of this work are:

- The model reproduces the PDF and scaling of observed lead fraction in the Central Arctic very well. It is not clear to which extent the differences between simulated and observed lead fractions are due to model or observation deficiencies.
- The model shows a clear multifractal scaling of the simulated heat fluxes in the Central Arctic. This scaling was shown to originate in the formation of leads.
- The mean heat flux is preserved across different model resolutions.
- The simulated lead-fraction and heat-flux scaling is not preserved across different model resolutions. This is most likely due in part to the misrepresentation of sub-grid scale heterogeneity in the current model ice thickness distribution.

Code and data availability. The lead fraction data set was not made publicly available when the original paper was published. The authors will provide copies of this data on request. The source code to neXtSIM is not yet publicly available, but the code will be made available upon request, pending usage restrictions.

Author contributions. EO and PR developed the scientific questions and analysis approach. EO performed the model runs and analysis and wrote the bulk of the text with PR and VD giving substantial input on the interpretation of results and the final text.

Competing interests. The authors declare that they have no conflict of interest.

Acknowledgements. This work was supported by the FRASIL (RCN #263044) and Nansen Legacy (RCN #276730) projects, financed by the Norwegian Research Council and the AOI project, financed by the Bjerknes Center for Climate Research.

References

Aagaard, K., Coachman, L., and Carmack, E.: On the halocline of the Arctic Ocean, Deep Sea Research Part A. Oceanographic Research Papers, 28, 529 – 545, https://doi.org/10.1016/0198-0149(81)90115-1, 1981.

Andreas, E. and Murphy, B.: Bulk transfer coefficients for heat and momentum over leads and polynyas, J. Phys. Ocean., 16, 1875–1883, 1986.

Andreas, E. L. and Cash, B. A.: Convective heat transfer over wintertime leads and polynyas, Journal of Geophysical Research: Oceans, 104, 25 721–25 734, https://doi.org/10.1029/1999JC900241, 1999.

Andreas, E. L., Paulson, C. A., William, R. M., Lindsay, R. W., and Businger, J. A.: The turbulent heat flux from arctic leads, Boundary-Layer Meteorology, 17, 57–91, https://doi.org/10.1007/BF00121937, 1979.

Barthélemy, A., Fichefet, T., Goosse, H., and Madec, G.: Modeling the interplay between sea ice formation and the oceanic mixed layer: Limitations of simple brine rejection parameterizations, Ocean Modelling, 86, 141 – 152, https://doi.org/10.1016/j.ocemod.2014.12.009, 2015.

Bouillon, S. and Rampal, P.: On producing sea ice deformation data sets from SAR-derived sea ice motion, The Cryosphere, 9, 663–673, https://doi.org/10.5194/tc-9-663-2015, 2015a.

Bouillon, S. and Rampal, P.: Presentation of the dynamical core of neXtSIM, a new sea ice model, Ocean Modelling, 91, 23–37, 2015b.

Bröhan, D. and Kaleschke, L.: A Nine-Year Climatology of Arctic Sea Ice Lead Orientation and Frequency from AMSR-E, Remote Sensing, 6, 1451–1475, 2014.

Bromwich, D. H., Wilson, A. B., Bai, L.-S., Moore, G. W. K., and Bauer, P.: A comparison of the regional Arctic System Reanalysis and the global ERA-Interim Reanalysis for the Arctic, Quarterly Journal of the Royal Meteorological Society, 142, 644–658, https://doi.org/10.1002/qj.2527, 2016.

Chechin, D. G., Makhotina, I. A., Lüpkes, C., and Makshtas, A. P.: Effect of Wind Speed and Leads on Clear-Sky Cooling over Arctic Sea Ice during Polar Night, Journal of the Atmospheric Sciences, 76, 2481–2503, https://doi.org/10.1175/JAS-D-18-0277.1, 2019.

Dansereau, V., Weiss, J., Saramito, P., and Lattes, P.: A Maxwell elasto-brittle rheology for sea ice modelling, The Cryosphere, 10, 1339–1359, https://doi.org/10.5194/tc-10-1339-2016, 2016.

Esau, I. N.: Amplification of turbulent exchange over wide Arctic leads: Large-eddy simulation study, Journal of Geophysical Research: Atmospheres, 112, https://doi.org/10.1029/2006JD007225, d08109, 2007.

Girard, L., Bouillon, S., Weiss, J., Amitrano, D., Fichefet, T., and Legat, V.: A new modelling framework for sea ice mechanics based on elasto-brittle rheology, Ann. Glaciol., 52(57), 123–132, 2011.

Gultepe, I., Zhou, B., Milbrandt, J., Bott, A., Li, Y., Heymsfield, A., Ferrier, B., Ware, R., Pavolonis, M., Kuhn, T., Gurka, J., Liu, P., and Cermak, J.: A review on ice fog measurements and modeling, Atmospheric Research, 151, 2 – 19, https://doi.org/10.1016/j.atmosres.2014.04.014, sixth International Conference on Fog, Fog Collection and Dew, 2015.

Hibler, W. D.: A dynamic thermodynamic sea ice model, J. Phys. Ocean., 9, 817–846, 1979.

Hutchings, J. K., Roberts, A., Geiger, C. A., and Richter-Menge, J.: Spatial and temporal characterization of sea-ice deformation, Ann. Glaciol., 52, 360–368, 2011.

Hutter, N., Losch, M., and Menemenlis, D.: Scaling Properties of Arctic Sea Ice Deformation in a High-Resolution Viscous-Plastic Sea Ice Model and in Satellite Observations, Journal of Geophysical Research: Oceans, 123, 672–687, https://doi.org/10.1002/2017JC013119, 2018.

Ivanova, N., Rampal, P., and Bouillon, S.: Error assessment of satellite-derived lead fraction in the Arctic, The Cryosphere, 10, 585–595, https://doi.org/10.5194/tc-10-585-2016, 2016.

Kagan, Y. Y.: Fractal dimension of brittle fracture, Journal of Nonlinear Science, 1, 1–16, 1991.

Koldunov, N. V., Danilov, S., Sidorenko, D., Hutter, N., Losch, M., Goessling, H., Rakowsky, N., Scholz, P., Sein, D., Wang, Q., and Jung, T.: Fast EVP Solutions in a High-Resolution Sea Ice Model, Journal of Advances in Modeling Earth Systems, 11, 1269–1284, https://doi.org/10.1029/2018MS001485, 2019.

Kozo, T. L.: Initial model results for Arctic mixed layer circulation under a refreezing lead, Journal of Geophysical Research: Oceans, 88, 2926–2934, https://doi.org/10.1029/JC088iC05p02926, 1983.

Kwok, R., Cunningham, G. F., Wensnahan, M., Rigor, I., Zwally, H. J., and Yi, D.: Thinning and volume loss of the Arctic Ocean sea ice cover: 2003–2008, Journal of Geophysical Research: Oceans, 114, https://doi.org/10.1029/2009JC005312, c07005, 2009.

Leppäranta, M.: The Drift of Sea Ice, Springer, Helsinki, 2005.

Li, X., Krueger, S. K., Strong, C., Mace, G. G., and Benson, S.: Midwinter Arctic leads form and dissipate low clouds, Nature Communications, 11, 206, https://doi.org/10.1038/s41467-019-14074-5, 2020.

Lüpkes, C., Gryanik, V. M., Witha, B., Gryschka, M., Raasch, S., and Gollnik, T.: Modeling convection over arctic leads with LES and a non-eddy-resolving microscale model, J. Geophys. Res., 113, C09 028, https://doi.org/10.1029/2007JC004099, 2008a.

Lüpkes, C., Vihma, T., Birnbaum, G., and Wacker, U.: Influence of leads in sea ice on the temperature of the atmospheric boundary layer during polar night, Geophys. Res. Lett., 35, https://doi.org/10.1029/2007GL032461, 2008b.

Marcq, S. and Weiss, J.: Influence of sea ice lead-width distribution on turbulent heat transfer between the ocean and the atmosphere, The Cryosphere, Volume 6, Issue 1, 2012, pp. 143-156, 6, 143–156, 2012.

Marsan, D. and Weiss, J.: Space/time coupling in brittle deformation at geophysical scales, Earth Planet. Sci. Lett., 296, 353–359, 2010.

Marsan, D., Stern, H. L., Lindsay, R., and Weiss, J.: Scale dependence and localization of the deformation of Arctic sea ice, Phys. Rev. Lett., 93, 178 501, 2004.

Matsushita, M.: Fractal Viewpoint of Fracture and Accretion, Journal of the Physical Society of Japan, 54, 857–860, https://doi.org/10.1143/JPSJ.54.857, 1985.

Maykut, G. A.: The surface heat and mass balance, in: The Geophysics of Sea Ice, edited by Untersteiner, N., NATO ASI Series, chap. 5, pp. 395–463, Springer US, 1986.

Morales Maqueda, M. A., Willmott, A. J., and Biggs, N. R. T.: Polynya Dynamics: a Review of Observations and Modeling, Reviews of Geophysics, 42, https://doi.org/10.1029/2002RG000116, 2004.

Morison, J. H. and McPhee, M. G.: Lead convection measured with an autonomous underwater vehicle, Journal of Geophysical Research: Oceans, 103, 3257–3281, https://doi.org/10.1029/97JC02264, 1998.

Morison, J. H., McPhee, M. G., Curtin, T. B., and Paulson, C. A.: The oceanography of winter leads, Journal of Geophysical Research: Oceans, 97, 11 199–11 218, https://doi.org/10.1029/92JC00684, 1992.

Nguyen, A. T., Menemenlis, D., and Kwok, R.: Improved modeling of the Arctic halocline with a subgrid-scale brine rejection parameterization, Journal of Geophysical Research: Oceans, 114, https://doi.org/10.1029/2008JC005121, c11014, 2009.

Rampal, P., Weiss, J., Marsan, D., Lindsay, R., and Stern, H.: Scaling properties of sea ice deformation from buoy dispersion analysis, Journal of Geophysical Research: Oceans, 113, https://doi.org/10.1029/2007JC004143, c03002, 2008.

Rampal, P., Bouillon, S., Ólason, E., and Morlighem, M.: neXtSIM: a new Lagrangian sea ice model, The Cryosphere, 10, 1055–1073, https://doi.org/10.5194/tc-10-1055-2016, 2016.

Rampal, P., Dansereau, V., Ólason, E., Bouillon, S., Williams, T., Korosov, A., and Samaké, A.: On the multi-fractal scaling properties of sea ice deformation, The Cryosphere, 13, 2457–2474, 2019.

Röhrs, J. and Kaleschke, L.: An algorithm to detect sea ice leads by using AMSR-E passive microwave imagery, The Cryosphere, 6, 343–352, 2012.

Rothrock, D. A. and Thorndike, A. S.: Measuring the Sea Ice Floe Size Distribution, J. Geophys. Res., 89, 6477–6486, 1984.

Sakov, P., Counillon, F., Bertino, L., Lisæter, K. A., Oke, P., and Korablev, A.: TOPAZ4: An ocean sea ice data assimilation system for the North Atlantic and Arctic, Ocean Sci., 8, 633–662, https://doi.org/10.5194/osd-9-1519-2012, 2012.

Schertzer, D. and Lovejoy, S.: Physical Modeling and Analysis of Rain and Clouds by Anisotropic Scaling Multiplicative Processes, J. Geophys. Res., 92, 9693–9714, 1987.

Smith, D. C. and Morison, J. H.: A numerical study of haline convection beneath leads in sea ice, Journal of Geophysical Research: Oceans, 98, 10 069–10 083, https://doi.org/10.1029/93JC00137, 1993.

Smith, D. C., Lavelle, J. W., and Fernando, H. J. S.: Arctic Ocean mixed-layer eddy generation under leads in sea ice, Journal of Geophysical Research: Oceans, 107, 17–1–17–17, https://doi.org/10.1029/2001JC000822, 2002.

Smith, J.: Oceanographic investigations during the AIDJEX lead experiment, AIDJEX Bull., 27, 125–133, 1974.

Spreen, G., Kwok, R., Menemenlis, D., and Nguyen, A. T.: Sea-ice deformation in a coupled ocean–sea-ice model and in satellite remote sensing data, The Cryosphere, 11, 1553–1573, https://doi.org/10.5194/tc-11-1553-2017, https://www.the-cryosphere.net/11/1553/2017/, 2017.

Stern, H. L. and Lindsay, R. W.: Spatial scaling of Arctic sea ice deformation, Journal of Geophysical Research: Oceans, 114, https://doi.org/10.1029/2009JC005380, c10017, 2009.

Stern, H. L., Stark, A. J., Zhang, J., Steele, M., and Hwang, B.: Seasonal evolution of the sea-ice floe size distribution in the Beaufort and Chukchi seas, Elementa Science of the Anthropocene, 6, https://doi.org/10.1525/elementa.305, 2018.

Tamura, T. and Ohshima, K. I.: Mapping of sea ice production in the Arctic coastal polynyas, J. Geophys. Res., 116, 2011.

Tetzlaff, A., Lüpkes, C., and Hartmann, J.: Aircraft-based observations of atmospheric boundary-layer modification over Arctic leads, Quarterly Journal of the Royal Meteorological Society, 141, 2839–2856, https://doi.org/10.1002/qj.2568, 2015.

Tonboe, R. T., Eastwood, S., Lavergne, T., Sørensen, A. M., Rathmann, N., Dybkjær, G., Pedersen, L. T., Høyer, J. L., and Kern, S.: The EUMETSAT sea ice concentration climate data record, The Cryosphere, 10, 2275–2290, 2016.

Vihma, T., Pirazzini, R., Renfrew, I. A., Sedlar, J., Tjernström, M., Nygård, T., Fer, I., Lüpkes, C., Notz, D., Weiss, J., Marsan, D., Cheng, B., Birnbaum, G., Gerland, S., Chechin, D., and Gascard, J. C.: Advances in understanding and parameterization of small-scale physical processes in the marine Arctic climate system: a review, Atmos. Chem. Phys. Discuss., 13, 32 703–32 816, 2013.

Wang, Q., Danilov, S., Jung, T., Kaleschke, L., and Wernecke, A.: Sea ice leads in the Arctic Ocean: Model assessment, interannual variability and trends, Geophysical Research Letters, 43, 7019–7027, https://doi.org/10.1002/2016GL068696, 2016.

Warren, S. G., Rigor, I. G., Untersteiner, N., Radionov, V. F., Bryazgin, N. N., Aleksandrov, Y. I., and Colony, R.: Snow Depth on Arctic Sea Ice, Journal of Climate, 12, 1814–1829, https://doi.org/10.1175/1520-0442(1999)012<1814:SDOASI>2.0.CO;2, 1999.

Weiss, J.: Scaling of Fracture and Faulting of Ice on Earth, Surveys in Geophysics, 24, 185–227, https://doi.org/10.1023/A:1023293117309, 2003.

Weiss, J. and Dansereau, V.: Linking scales in sea ice mechanics, Philosophical Transaction Royal Society A: Mathematical, Physical and Engineering Sciences, 375, 20150 352, https://doi.org/10.1098/rsta.2015.0352, 2017.

Weiss, J. and Marsan, D.: Scale properties of sea ice deformation and fracturing, CR Phys., 5, 735–751, 2004.

Willmes, S. and Heinemann, G.: Pan-Arctic lead detection from MODIS thermal infrared imagery, Annals of Glaciology, 56, 29–37, https://doi.org/10.3189/2015AoG69A615, 2015.

Winsor, P. and Björk, G.: Polynya activity in the Arctic Ocean from 1958 to 1997, Journal of Geophysical Research: Oceans, 105, 8789–8803, https://doi.org/10.1029/1999JC900305, 2000.

Winton, M.: A reformulated three-layer sea ice model, J. Atm. Ocean.Tech., 17, 525–531, 2000.